Electronic supplementary information (ESI)

Multi-mode Mechanoluminescence of Fluoride Glass Ceramics from Rigid to Flexible Medium Toward Multi-Scene Mechanical Sensor

*Yingdan Song [a,b,c], Jianqiang Xiao [b], Lei Zhao [a,c] *, Zhichao Liu [b], Yami Ling [a,c], Yingjuan Yan [a,c], Yixuan Xu [a,c], Alexey·Nikolaevich Yakovlev [d], Tingting Hu [d], Tatiana Grigorievna Cherkasova [d], Qiang Xu [a,c]*, Canjun Wang [a]*, Xuhui Xu [b]**

[a] *School of Physics and Opto-Electronic Technology, Baoji University of Arts and Sciences, Baoji, Shaanxi, 721016, P.R. China*

[b] *College of Materials Science and Engineering, Kunming University of Science and Technology, Kunming 650093, P. R. China*

[c] *Baoji Key Laboratory of Micro-Nano Optoelectronics and Terahertz Technology, Baoji, Shaanxi, 721016, P.R. China*

[d] *T.F. Gorbachev Kuzbass State Technical University, Kemerovo, 650000, Russia.*

* *Corresponding Authors' Email:*

zhaoleibjwl@163.com (Lei Zhao);

xuqiang@bjwlxy.edu.cn (Qiang Xu);

cjwangbj@126.com (Canjun Wang);

xuxuh07@126.com (Xuhui Xu).

Electronic supplementary information (ESI) available.

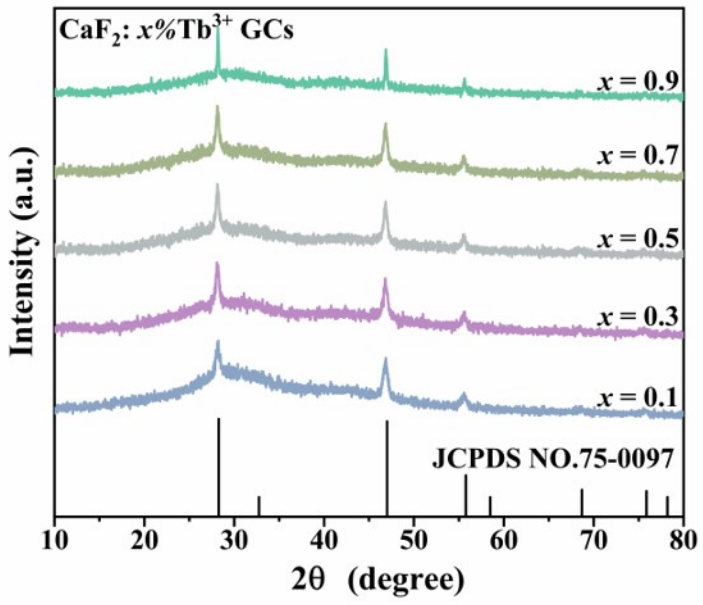

Fig. S1. XRD patterns of CaF_2: x%Tb^{3+} GCs（x = 0.1, 0.3, 0.5, 0.7, 0.9）.

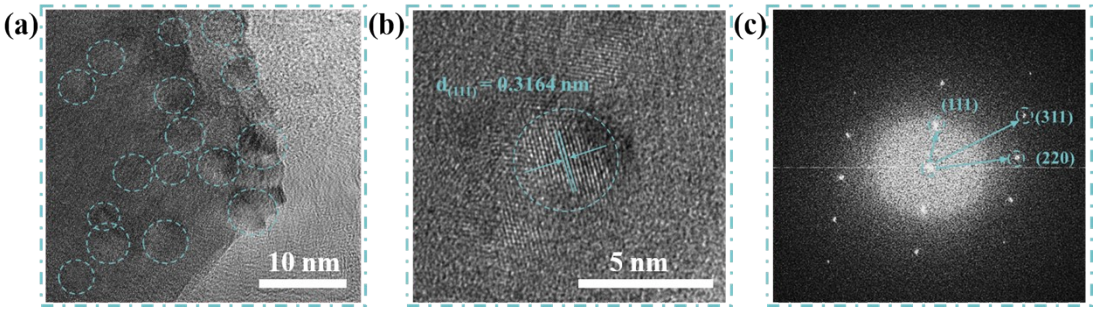

Fig. S2. CaF_2: 0.7%Tb^{3+} GCs **(a)**TEM image. **(b)**HAADF-STEM image. **(c)**the corresponding FFT image.

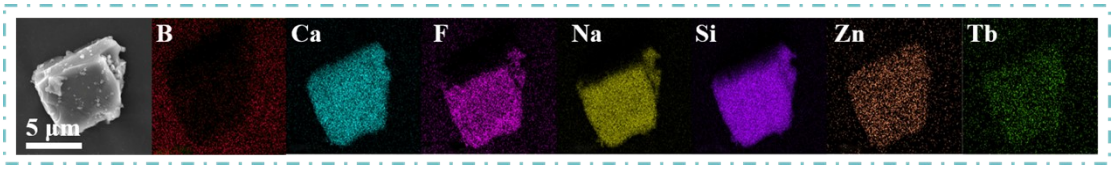

Fig. S3. SEM and EDS Mapping images of CaF_2: 0.7%Tb^{3+} GCs.

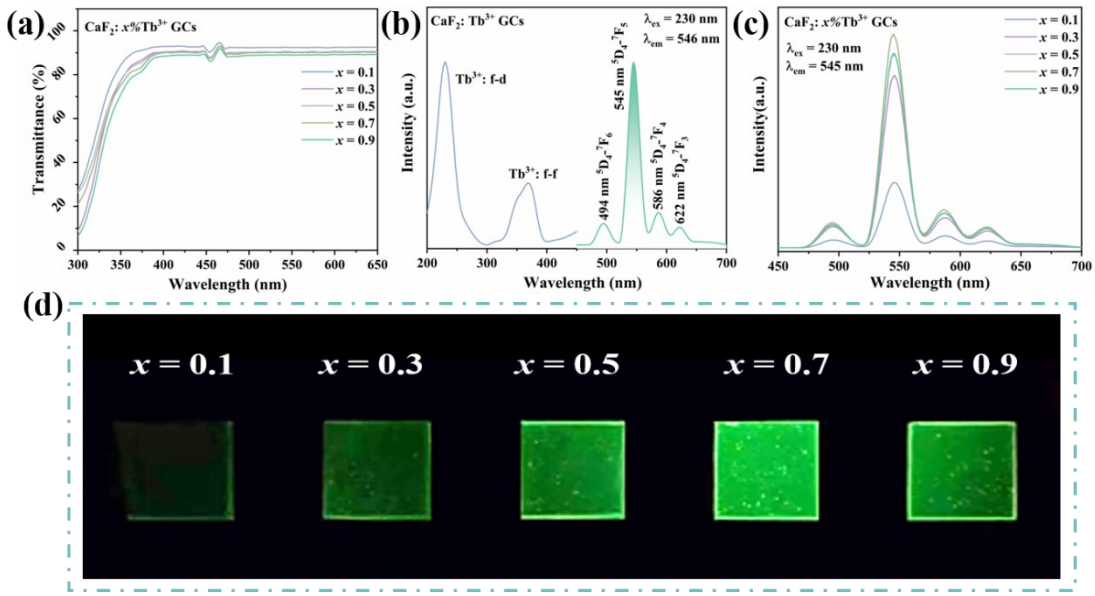

Fig. S4. (a) Transmissivity spectra, **(b)** PL and PLE spectra, **(c)** Series PL spectra, **(d)** Series of PL photos under 365 nm UV light of CaF_2: x%Tb^{3+} GCs（x = 0.1, 0.3, 0.5, 0.7, 0.9).

The optical properties of CaF_2: x%Tb^{3+} GCs (x = 0.1, 0.3, 0.5, 0.7, 0.9) are characterized in **Fig. S4**. **Fig. S4(a).** shows the transmittance spectra of CaF_2 doping with different concentrations of Tb^{3+} ions, and it can be seen that all samples have a high transparency of more than 80%. **Fig. S4(b)** shows its optimal PLE and PL spectra, and it can be observed that the optimal excitation wavelength is 230 nm and the emission wavelength is 545 nm, thus monitoring the measured 200 -700 nm PLE-PL spectra, the sample consists of four emission bands, belong to 494, 545, 586, 621 nm, corresponding to the energy level transitions of $^5D_4$ - $^7F_6$, $^5D_4$ - $^7F_5$, $^5D_4$ - $^7F_4$, $^5D_4$ - $^7F_3$, PL spectrum of samples with different doping concentrations of Tb^{3+} is shown in **Fig. S4(c)**, it can be seen that the Tb^{3+} doping concentration of 0.7% PL intensity reaches its maximum and then decreases due to the concentration quenching effect, while PL photos under 365 nm UV light are given in **Fig. S4(d)**.

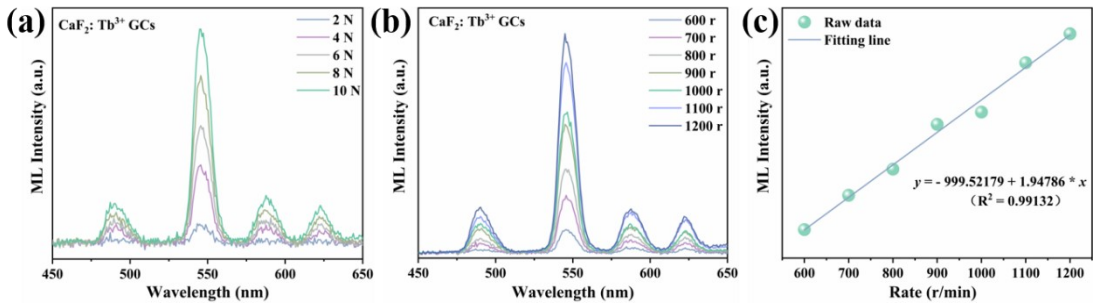

Fig. S5. (a) ML spectra of the CaF_2: Tb^{3+} GCs under different loads. **(b)** ML spectra of the CaF_2: Tb^{3+} GCs under different loading rates. **(c)** The relationship between ML intensity of CaF_2: Tb^{3+} GCs and applied rates.

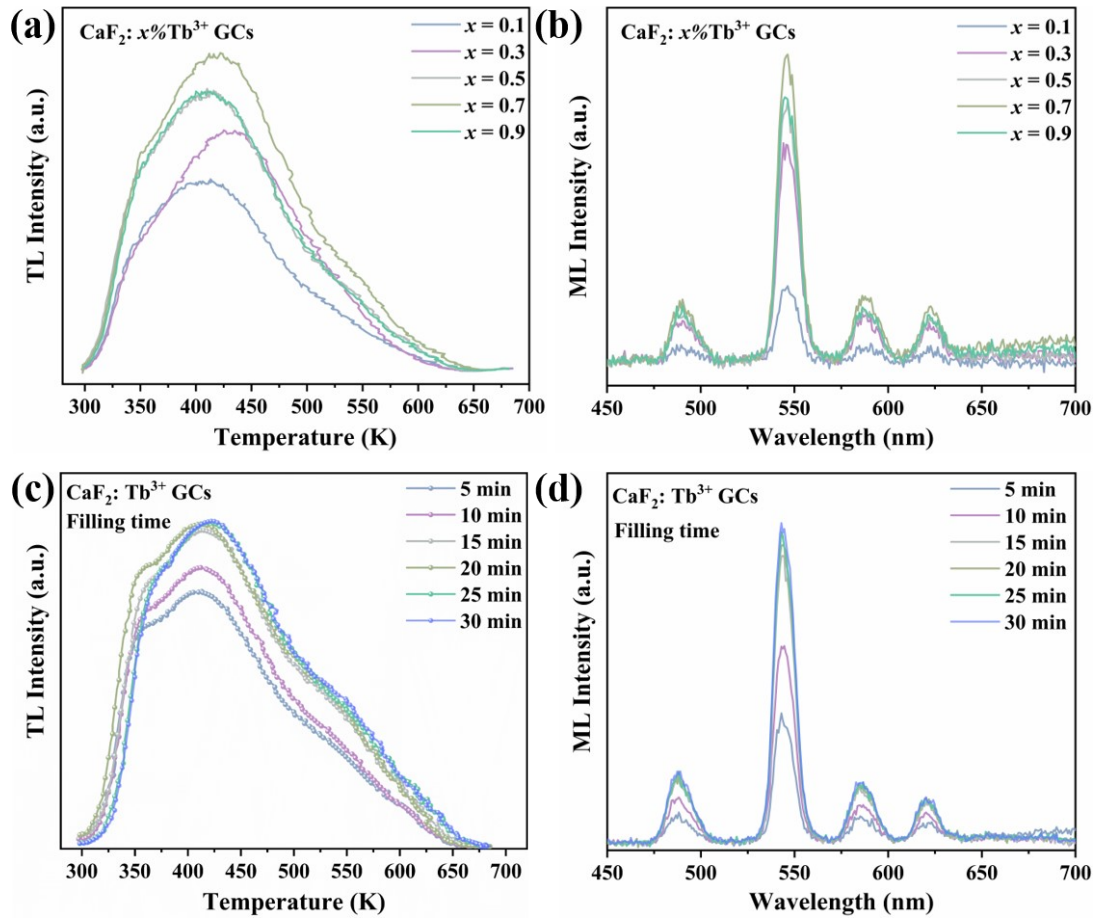

Fig. S6. CaF_2: x%Tb^{3+} GCs（x = 0.1, 0.3, 0.5, 0.7, 0.9）after X-Ray pre-irradiated for 15 min **(a)** TL curves. **(b)** ML spectra under X-Ray irradiation filling condition. **(c)** TL curves at different pre-irradiated times. **(d)** ML spectra at different pre-irradiated times.

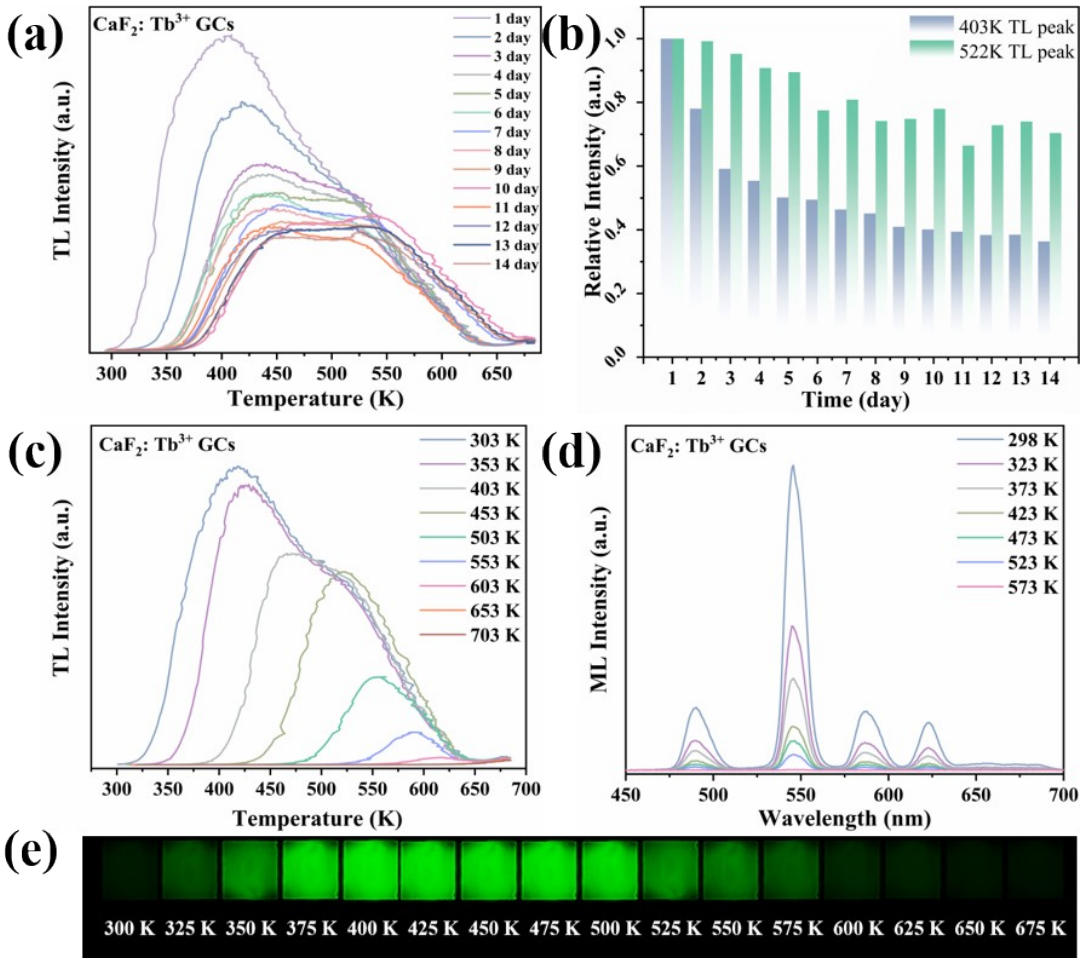

Fig. S7. (a) TL curves of CaF_2: 0.7%Tb^{3+} GCs placed at RT for different days. **(b)** The relationship of placed days and TL intensity. **(c)** Temperature-dependent TL curves after 15 min of X-Ray irradiation. **(d)** Temperature-dependent ML spectra after 15 min of X-Ray irradiation. **(e)** Temperature-dependent TL photos of the CaF_2: Tb^{3+} GCs.

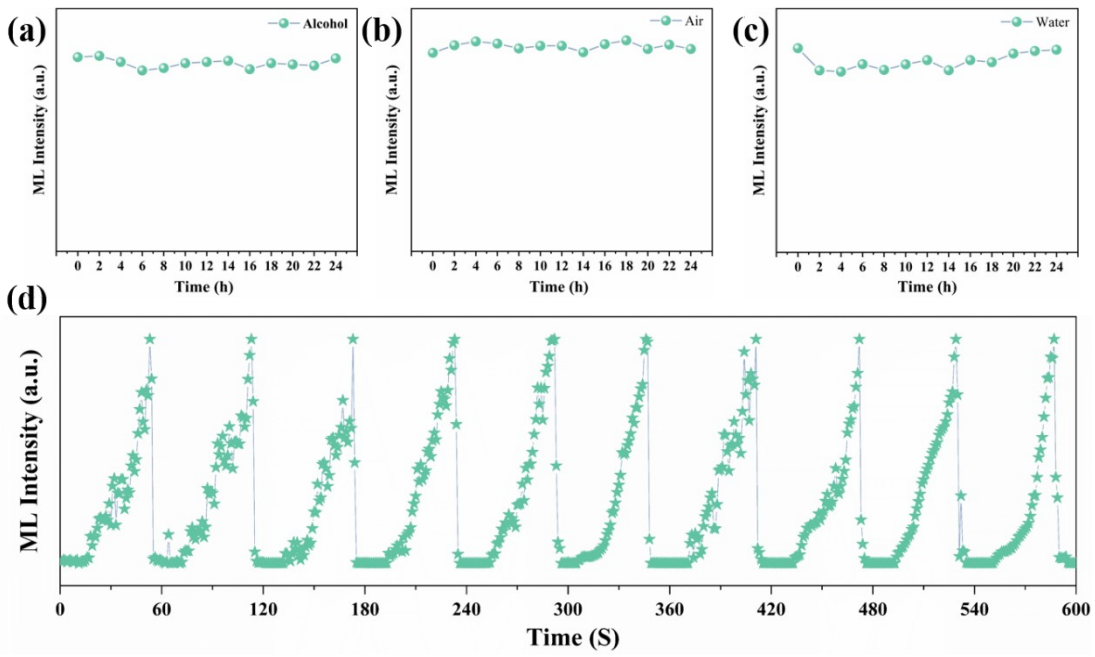

Fig. S8. CaF_2: 0.7%Tb^{3+} GCs **(a)** Stability of alcohol for 24 hours. **(b)** Stability in the air for 24 hours. **(c)** Stability in water for 24 hours. **(d)** ML intensity of 10 consecutive friction cycles after 15 minutes of X-Ray irradiation.

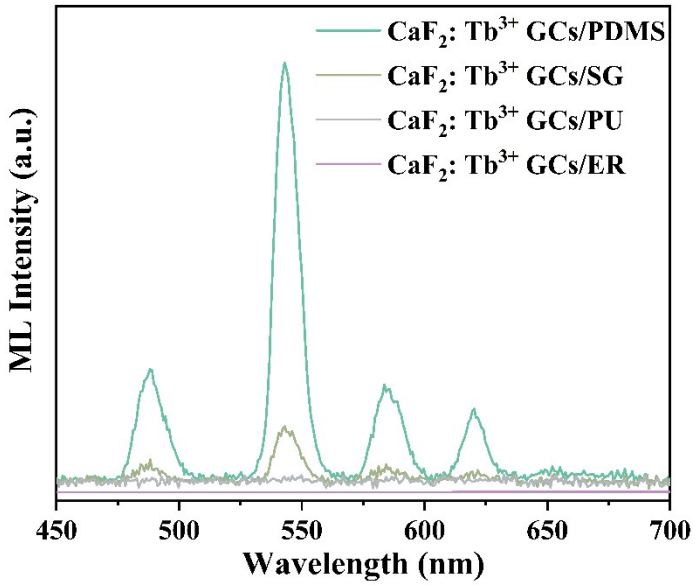

Fig. S9. ML spectra of CaF_2: Tb^{3+} GCs powder in different mediums.